Structural Characterization of an Ordered Aromatic Polyimide: Pyromellitic Dianhydride–Oxydianiline

Tze W. Poon,† Ravi F. Saraf,*‡ and B. David Silverman‡

T. J. Watson Research Center, IBM Research, Yorktown Heights, New York 10598, and Department of Materials Science, The University of Texas, Austin, Texas 78752

Received December 14, 1992; Revised Manuscript Received March 22, 1993

ABSTRACT: The three-dimensional (3-D) ordered structure of semiflexible pyromellitic dianhydride oxydianiline (PMDA–ODA) is calculated using the CHARMM molecular modeling program. Polymorphism in the ordered chain conformation is calculated with chain periodicities $n = 2$, 3, and 4, where n is the number of monomers within the period. A planar zigzag chain cross-section is observed in the $n = 2$ and 4 structures while a triangular cross-section is observed in the $n = 3$ structure. The optimum ordered chains are packed to form a 3-D crystal by considering relative chain translations parallel and perpendicular to the chain axis by adjusting the number of basis chains, m in the unit cell. Although the $n = 3$ and 4 periodicities have not been reported, we calculate an approximate 3-D crystal structure factor. Corresponding structure factors along and perpendicular to the chain are calculated and compared with wide-angle X-ray scattering experiments, with good agreement. The lowest energy 3-D structure consists of an $n = 2$ conformation, with single chain periodicity along the interplanar packing direction and double chain periodicity along the edge-on stacking direction.

I. Introduction

Due to their thermal stability, high glass transition temperature, low thermal expansivity, good mechanical properties, and low dielectric constant, polyimides (PIs) have found significant applications in the microelectronics and aerospace industries. Their easy processibility in precursor states to form smooth (average roughness <1 nm) thin films has made them an attractive dielectric material for multilayer chip packaging modules in microelectronics and potential matrix material for high-performance composites in the aerospace industry. To achieve optimum properties for the applications previously mentioned, it is important to establish (chemical and molecular) structure–property relationships in polyimides, as demonstrated by previous works.[1-5] In particular, chain flexibility and packing induced by tailoring the chemical structure of the chain have been shown to strongly affect material properties such as the thermal expansivity and elastic modulus.[6-10] These features are established by observing the changes in properties through the alteration of chain rigidity and structure with various flexible main-chain spacers and side groups. Furthermore, the PI's are composed of two phases, viz., the mesomorphic ordered phase (MOP) and the liquid-like amorphous phase (LAP), as observed in other semicrystalline polymers. The quantification of weight or volume fraction of the two phases, or the percentage of crystallinity, is important in characterizing material properties.

In this paper, we model the molecular structure for the MOP of the pyromellitic dianhydride–oxydianiline (PMDA–ODA) polyimide. The ordered conformation and three-dimensional packing at 0 K is obtained through the CHARMM molecular modeling software.[11] Enthalpic energy minimization with empirical potentials is utilized. The corresponding structure factor is calculated and compared to wide-angle X-ray scattering (WAXS) data. Peaks associated with chain morphology (the (00l) and (002l) reflections) and the chain packing are consistent with experiments. In addition, the origins of some peaks are also identified. Other molecular features of the MOP have been discussed previously along with other polyimides.[12] Here we will only point out the highlights. Examining the torsional environment between adjacent aromatic units of the chain, we found that there are two independent chains, each with two repeat monomer units in the primitive unit cell of PMDA–ODA. The density of the calculated MOP can be used to calculate the percentage of observed crystallinity. Furthermore, the structure of this phase can be used to understand, predict, and tailor the material properties of films made with this PI.

II. Model

Calculation Procedure. Modeling of the PMDA–ODA structure is carried out utilizing the molecular modeling software CHARMM.[11] (See ref 11 for more details of the software.) The calculation is broken into three parts. First, the lowest enthalpic energy conformation of a single chain is determined. The coordinate system is chosen such that the polymer chain is lying along the z axis. Second, a two-dimensional monolayer is constructed by replicating a single chain along the direction perpendicular to the chain axis (y axis). The lowest energy structure is obtained by perturbing the interchain distance and chain conformation, while keeping an identical conformation for all chains. Under this constant, neighboring planar units can still translate and/or rotate with respect to each other with the backbone of the chain possessing some degree of curvature. Third, the energy-minimized 2-D monolayers are stacked along the x axis to produce a 3-D structure. Appropriate degrees of freedom (x,y,z translations and rotations and chain conformation) are allowed to yield the lowest enthalpic energy structure. All the energies in this paper are quoted on a per-monomer basis unless specified. While identical chain conformations are kept within a layer, no constrain is imposed between neighboring layers.

To obtain the minimum enthalpic energy conformation, a single polymer chain with 40 monomer units is constructed and allowed to relax without constraint. The resultant structures, dependent upon the initially chosen geometries, possess periodicities consisting of 2, 3, 4, or 6 monomer units. In constructing the unit cell, the number of monomer units n are chosen with values from 2 to 6. The corresponding axial length (i.e., period) of the lattice

* To whom correspondence should be addressed.
† The University of Texas.
‡ IBM Research.

0024-9297/93/2226-3369$04.00/0

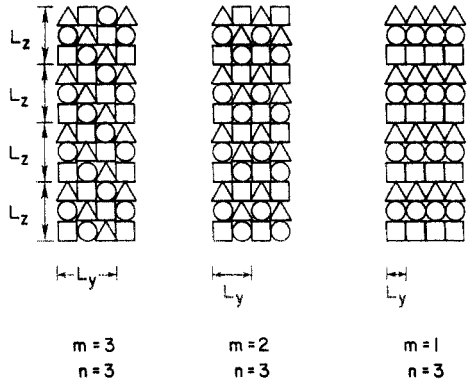

Figure 1. Possible structures of monolayer calculated from m = 3 chain ensemble, where each chain has n = 3 monomer periodicity. The two constraints imposed on the chains are n = 3 for each chain and identical chain conformation for all three basis chains.

Table I. Relative Energies of PMDA-ODA n = 3 Monolayer with Various Number of Independent Chains Assigned

	energy	
no. of chains	kcal/mol	eV/monomer
1	0	0
2	0.72	0.03
3	1.22	0.05

basis is L_z. Although the chains in the crystalline phase can possess one or all of these periodicities, a given ordered structure contains only one type of chain conformation in this study. The chain with n = 2 will be shown to have the lowest energy. Furthermore, its coherence length, c, along the chain axis will be shown to agree with the wide-angle X-ray scattering (WAXS) data.

Next, a semiinfinite monolayer is constructed. Chains with prescribed n monomer units (with a periodicity L_z) are chosen with their axes aligned with the z axis. The entire ensemble is then replicated along the y axis with proper coordinate translations along this axis. A single layer is thus generated in the yz plane. The search for a minimum conformational enthalpic energy structure is carried out under the constraint of appropriate periodic boundary condition (PBC). The PBC along the z axis is imposed by keeping n constant. A periodicity in interchain packing is also expected in an ordered structure. A monolayer is constructed by repeating a group of m chains along the y axis with lateral dimension L_y. The m chains in the cell are allowed to relax, and the conformations can change independent of each other. This implies that the interchain distance can be altered. The chains can slide with respect to each other and can adopt different conformations. Consider m = 3 chains in the calculation cell, each having n = 3 monomers per repeat unit. Figure 1 shows some typical structures that may arise. We know in this example that although the calculation may start with m = 3, the structure may converge to solution with $m \leq 3$. In this study, the lowest energy conformation of a monolayer contains only one chain (i.e., m = 1). The identical chain conformation has a face-to-face stacking of the neighboring dianhydride and diamine planar units. It is noted that packing of other structures with $m \geq 1$ shows minor deviations from this ideal face-to-face stacking. Nevertheless, the chains remain nominally identical. The relative energy differences (using the lowest energy structure as reference) listed in Table I show a maximum deviation of ~0.05 eV per monomer (0.0013 eV/atom). This is only 5% of the thermal energy at 300 K and is therefore insignificant. We therefore conclude that the

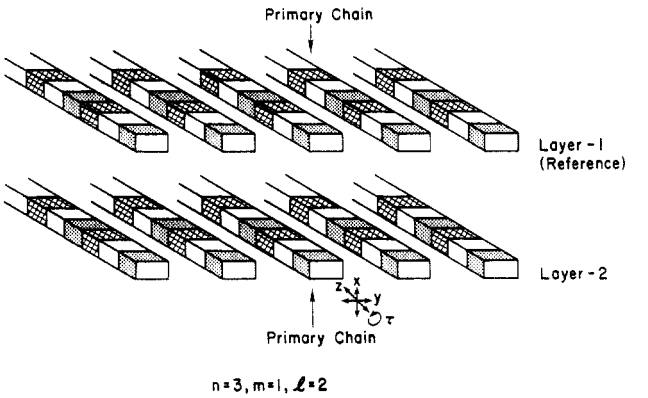

Figure 2. Bilayer calculated from two monolayers, each composed of m = 1 in L_y. The two basis chains are allowed to translate and rotate with respect to each other.

m = 1 chain exhibits one possible periodicity along the packing direction of the monolayer. Furthermore, m = 1 indicates the conformations of neighboring chains are in perfect registry. This observation is consistent with other polymeric crystalline structures.[13]

Next, layers are stacked together to construct a 3-D structure. Since the chain conformation is defined by choosing n = 2, 3, 4, or 6 and m = 1 is sufficient to define a monolayer, a bilayer can be constructed by assigning two independent chains in the two different monolayers, i.e., l = 2, in the calculation cell of thickness L_x. The two monolayers in the cell can translate and rotate independently as schematically shown in Figure 2. We set the initial condition such that the two chains are separated far enough (≥10 Å) in the x direction to allow for relative rotation and translation as the monolayers approach each other during structural relaxation. Similarly, structures with more than two layers can be constructed by assigning one independent chain per monolayer. An infinite 3-D structure is then constructed by applying the PBC along the x direction. The number of atoms in the primitive cell as well as the number of image atoms generated by the PBC increases drastically with an increase in the distinct number of monolayers assigned in the calculation cell. For example, the calculation of atom-pair interactions requires 26 images of the primitive calculation cell under 3-D PBC, compared to 8 images in the 2-D case. The extra computational burden severely limits the number of atoms that can be assigned, making the modeling of a few distinct monolayers improbable under the current computational resources. Since most interactions (excluded volume, van der Waals, etc.) are short range (first neighbor) in nature, 2–3 layers may be sufficient to represent the ideal 3-D infinite crystalline structure. The electrostatic interaction in 3-dimensions requires long-range convergence to be treated properly; however, in the present calculation this interaction is neglected. The present model, at least, yields the short-range packing preferred under the constraints imposed by the short-range repulsive excluded volume interactions. At present we perform calculations for only bi- and trilayer structures. In cases where an infinite 3-D structure is required, we take the relaxed bi- or trilayer structure and replicate it with appropriate coordinate translations along the x direction. We adopt this strategy instead of applying the PBC in the x direction. The unit length L_x needed for the density calculation is taken as the averaged coordinate differences $\langle \Delta x \rangle$ of the centers of mass of corresponding planar units in neighboring monolayers.

Scattering Pattern. Static structural factors of the generated ordered structures are calculated and compared

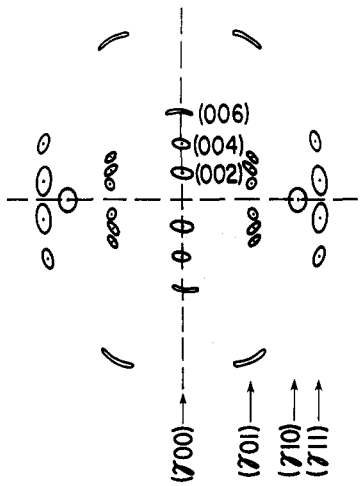

Figure 3. Schematic of WAXS reported by Gardner *et al.*[17]

with wide-angle X-ray scattering patterns. Polyimide films made by conventional methods are textured: For spun-cast films, the polymer chains lie parallel to the surface, giving a planar texture.[14] For fiber-drawn films, the chains are aligned parallel to the draw axis, giving a fiber texture.[15] To compare the experimental observations with the calculated structures, a cylindrical averaged scattering pattern is calculated by rotating the structure factors around the chain axis by 360° in 1° increments. The results are discussed in terms of layer lines. The meridional reflection (00*l*) and the first three layer lines are reported and analyzed to demonstrate the validity of the modeled structures. The calculated scattering patterns is compared to the fiber pattern obtained experimentally by Gardner *et al.*,[17] schematically shown in Figure 3. All atoms are stationary (i.e., no Debye–Waller line broadening is considered) and no X-ray absorption is considered. Furthermore, to reduce the line broadening due to finite size, a large cell in all three directions is used to calculate the structure factor. The cell is constructed by translating L_x, L_y, and L_z, the cell lengths utilized in the density calculation.

For the meridional scattering pattern, only the replication of the calculation cell along the z direction is performed. It is observed that the structure factor does not change significantly for polymer chains with 12–20 monomer units. The cylindrical average is obtained on a bundle of 8–10 chains. For equatorial scattering (i.e., the zeroth layer line) and the first two layer-line patterns, replication of the calculation cell is performed along all three directions (x, y, and z). It is also found that an ensemble of 10 by 10 chains, each having 4 monomer repeat units is adequate for this calculation. Good statistics with no significant edge effects up to the second layer line is obtained for a reasonable computational time.

III. Results and Discussion

The energy, the repeat length projected onto the polymer chain axis, c, and the density, ρ, of the modeled bi- and trilayer crystalline structure with n = 2–6 are listed in Table II. For the bilayers, the n = 2 structure possesses the lowest energy. Other structures show nominally higher values. The largest energy difference is between the n = 2 and n = 3 structures. The difference is merely 0.13 eV per monomer (3.09 kcal/mol), corresponding to $^1/_{10}$ the thermal energy of each atom at 300 K. For the trilayers, the n = 2 structure also possesses the lowest energy. The trilayer has more nonbinding interaction energies than the bilayer, and thus energies corresponding to the two

Table II. Relative Energies of Bi- and Trilayer Structures with Various Number of Repeat Units Assigned to the Chain

	energy			
repeat units	kcal/mol	eV/monomer	c[a] (Å)	ρ (g/cm^3)
		Bilayer Structures		
2	0	0	16.43	1.515 ± 0.033
3	3.09	0.13	15.78	1.512 ± 0.024
4	1.00	0.04	15.12	1.523 ± 0.466
6	1.96	0.09	15.67	1.534 ± 0.084
		Trilayer Structures		
2	0	0	16.43	1.513 ± 0.028
3	0.21	0.01	16.31	1.545 ● 0.040

[a] c is the repeat length projected onto the fiber axis.

systems cannot be compared. The small energy difference for bilayer structures suggests that it is possible for PMDA–ODA to form a crystalline phase with a variety of repeat units (i.e., n) along the chain. This may be one reason that the ordered structure is liquid-crystalline-like.[1] The coherence length, given as c/n, ranges from 15.12 to 16.43 Å for all structures. This is comparable to the experimentally observed value. The measured value of 16.2 Å[2-4] falls between the two values obtained for the n = 2 and n = 3 (bilayer) structures, indicating the possibility of significant variation in the conformation. Variations in coherence length have also been observed due to interfacial effects[4] and stretching.[16] Grazing incident X-ray scattering (GIXS) measurements have indicated a variation from 15.7 to 16.1 Å. The variation due to chain distortion from applying tension is significantly larger.[16] Furthermore, for various n's, variation in ρ is also observed. This is attributed to a change in the cross-sectional area and shape that will affect the chain packing. Figure 4 shows the various chain conformations and their corresponding cross-sections. The largest (1.534 g/cm^3) and lowest (1.512 g/cm^3) values correspond to n = 6 and 3 bilayers, respectively.

For the n = 2 structures, both bilayer and trilayer show identical values of c/n and p, indicating that two independent monolayers are sufficient to construct the 3-D crystal. The ρ value of 1.515 g/cm^3 is within a reasonable range. It is larger than those reported experimentally,[2,3] since the sample is always composed of a dense crystalline phase and less dense amorphous phase. For n = 3, both c/n and p show significant differences between the bi- and trilayers. To model the basis unit for the 3-D infinite structure, more layers have to be added to the calculation cell until asymptotic values for c and p are observed. Partly due to computational limitations and in light of the fact that the n = 2 structure has the lowest energy and corresponds to experimental observation,[17] we have investigated 3-D structures for n = 2 in greater detail than the other conformations. Instead we have analyzed some results that serve to compare the different chain conformations.

A perspective view of the n = 2 trilayer structure is shown in Figure 5. As has been discussed elsewhere in greater detail,[12] this structure exhibits a face-to-face packing of aromatic planar units with a separation of about 3.4 Å and a shift between neighboring units from 1.6 to 1.9 Å. The packing order between adjacent monolayers (the edge-on direction) has an averaged edge-on separation of 6.1 Å and a shift of 2.5 Å. The C–O–C angle of the ether linkage is between 121 and 125°. The torsional environment of the two neighboring monolayers is different. Thus the basic unit cell (primitive cell) contains two independent chains, with L_x = 13.2 Å, L_y = 3.86 Å, and L_z = 32.86 Å.

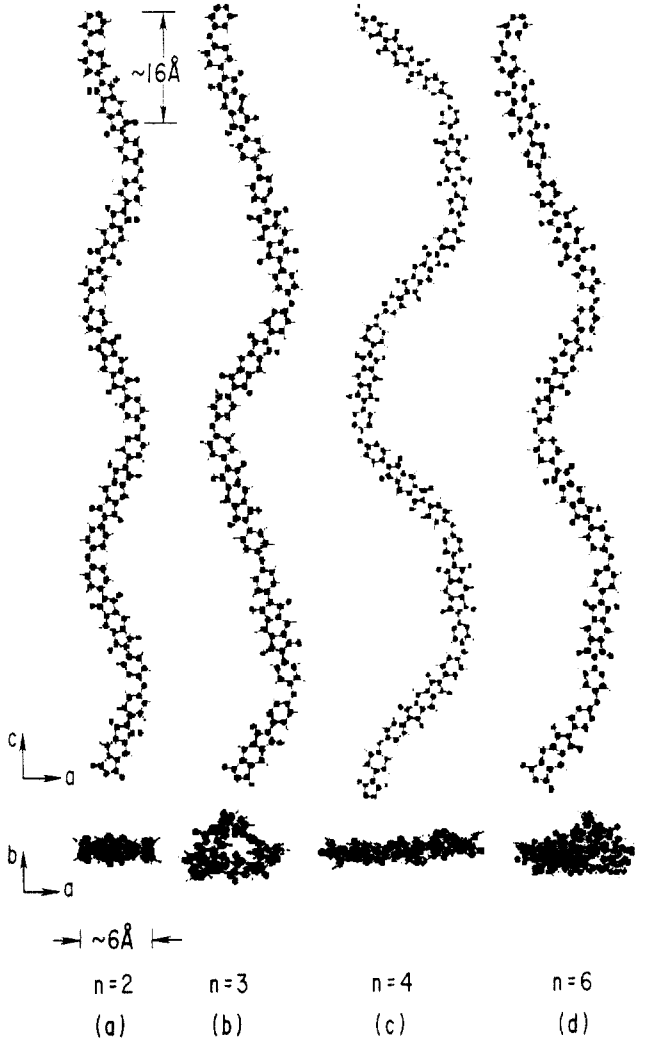

Figure 4. Chain conformations of $n = 2, 3, 4$, and 6 repeat units. $n = 2$ and 4 structures are planar-like as apparent from the cross-sectional view. $n = 3$ structure has a triangular cross-section, and $n = 6$ structure has both $n = 2$ and 3 like nature.

The three lattice constants are subsequently referred to as a, b, and c in the paper.

Cylindrically averaged scattering patterns from the static structural factors corresponding to the modeled structures have been generated and compared with WAXS. Figure 6 illustrates scattering at the meridian and equator. They provide information regarding the periodicity along the backbone and packing of neighboring chains. The Δq interval for the calculated structure factor in reciprocal space is ~ 0.034 Å^{-1}. The meridional line for the $n = 2$ bi- and trilayer structures shows eight peaks in the q range shown in Figure 6a,b, indicating a high degree of order in chain morphology. The peaks are (002) to (0,0,16) reflections, corresponding to a c/n value of ~ 16 Å. The $n = 3$ bilayer shows only the (003), (006), and (009) reflections (Figure 6c,d), while the trilayer shows sharper reflections with two higher order peaks, viz., (0,0,12) and (0,0,18). The corresponding ρ values (Table II) also indicate that the more ordered structure possesses a higher density for the trilayer compared to the bilayer for $n = 3$. In light of all the observations, it is reasonable to expect that the conformation of the backbone for various n's is close to the observed "ordered" structure.

Inspecting the torsion angles of various aromatic rings, it is observed that the $n = 2$ structure seems to be a 2/1 helix as signified by the symmetry in the torsion angles (Figure 7a,b). $n = 3$, however, is not a 3/1 helix due to the asymmetry in the torsion angles for the three anhydride groups shown in Figure 7d. The symmetry is not threefold

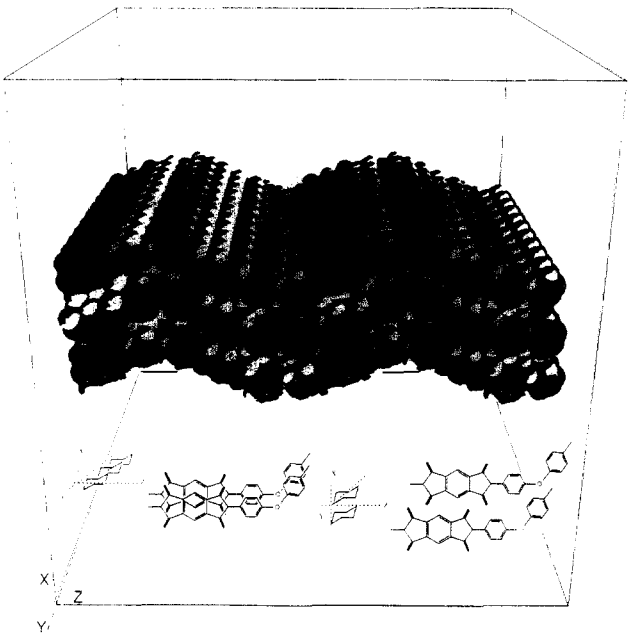

Figure 5. Perspective view of the $n = 2$ trilayer structure. Chains are stacked face-to-face and edge-on along the y and x (or b and a) axes, respectively, with their backbones lying along the z (or c) axis. Molecules are drawn with van der Waals space-filled model.

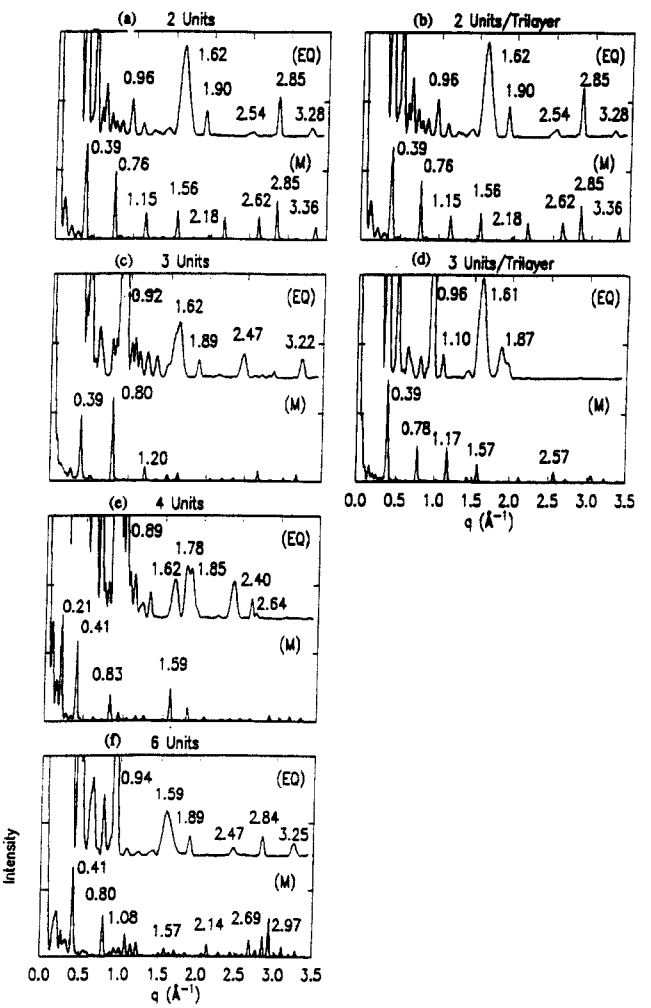

Figure 6. Equatorial and meridional scattering patterns. (a) and (b) correspond to $n = 2$ bi- and trilayer, (c) and (d) to $n = 3$ bi- and trilayer, and (e) and (f) to $n = 4$ and 6 bilayer, respectively.

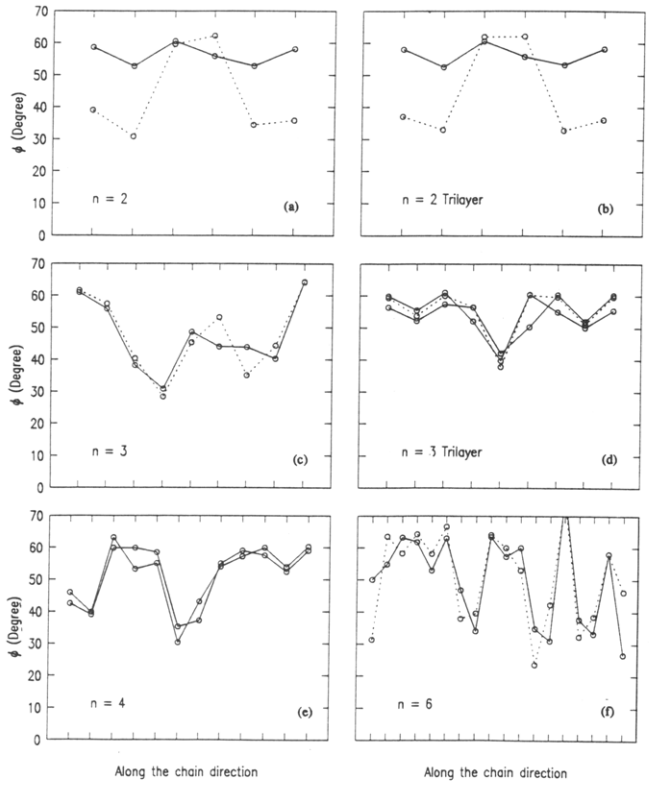

Figure 7. Relative torsion angles along the chains. (a) and (b) correspond to $n = 2$ bi- and trilayer, (c) and (d) to $n = 3$ bi- and trilayer, and (e) and (f) to $n = 4$ and 6 bilayer, respectively.

but twofold, implying that the helix does not have a direction (i.e., up or down). Comparing the bilayer (Figure 7c) and trilayer (Figure 7d), the torsion angle indicates that the former structure is not fully relaxed.

The meridional line for $n = 4$ in Figure 6e indicates an extra reflection at $q = 0.213$ Å^{-1}, unlike $n = 2$ and 3. The corresponding coherence length $c = 29.5$ Å is attributed to the planar nature of the conformation as opposed to the case for $n = 3$. The reason for the absence of higher order reflections is similar to that for the $n = 3$ structure; i.e., the calculation cell contains more than two layers along the x axis. The $2\pi/4$ rotation coupled with one-fourth pitch translation does not superimpose due to the complex tilt angles of the anhydride groups as shown in Figure 7e. The chain cross-section (Figure 4c) reveals a planar nature as the $n = 2$ structure, although with larger deviation.

The meridional line for $n = 6$ in Figure 6f reveals reflections at locations similar to those of the $n = 2$ and 3 conformations. The torsional environment (Figure 7f) has complex behavior since only a bilayer is considered. The chain cross-section (Figure 4d) seems to have both planar-like (as in $n = 2$) and nonplanar-like (as in $n = 3$) character. Judging from this complexity, we conjecture that the $n = 6$ structure may not possess long-range order. However, some of the local regions in the amorphous phase may be composed of this conformation. This would then be analogous to the superhelical structures of oriented atactic polystyrene observed by amorphous scattering.[18]

Observation of different conformations with comparable energies suggests the existence of a polymorphous nature of PMDA–ODA in the solid phase. It is conceivable that the material possesses one conformation predominantly ($n = 2$) and a small portion of the other n conformations. The degree of order, ranging from liquid crystalline to crystalline, may be determined by the persistence of the dominant conformation. It is possible that there is a crystalline phase composed mostly of the $n = 2$ conformation and a small amount of other n structures. This would lead to a range of repeat lengths c/n ranging from 15.1 to 16.4 Å. Furthermore, the increase in c from the bulk to the surface of a thin film[4] may be interpreted as consisting of more $n = 2$ conformation at the surface. The significant increase in c associated with the plastic deformation may also be related to a conformational transformation. This has been observed in several polymers such as PBT and polyallyne.[19]

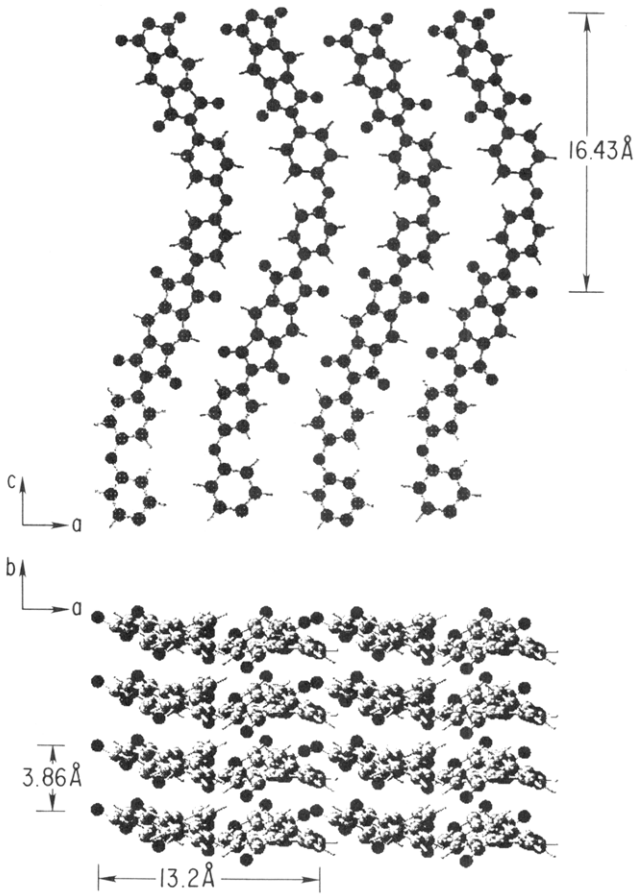

Figure 8. Schematic diagram illustrating the $n = 2$ structure. The ac and ab plane projections are shown in (a) and (b), respectively. The unit cell contains two chains with $a = 13.2$ Å and $b = 3.86$ Å.

Based on the fiber pattern obtained by Gardner *et al.*[17] with a strong (002) reflection, we have chosen the $n = 2$ conformation for further analysis. This conformation is illustrated in Figure 8. For clarity, only one monomer unit is indicated for the c-axis projection. The unit cell contains two chains per lattice (Figure 8a). Chains along the b axis are superimposed as seen in Figure 8b. However along the a axis, alternative chains are superimposable. Furthermore, from Figure 8, the a, b, and c axes are mutually perpendicular, implying an orthogonal unit cell with two chains per cell where $a = 13.20$ Å, $b = 3.86$ Å, and $c = 32.08$ Å. To analyze the origins of various reflections, we apply a uniform strain to the structure along the a and b axes in an incremental manner and observe the shifts in the reflections. The individual chain conformation is kept identical while stretching is applied. Thus only the spacing between neighboring chains is affected. Since the equatorial reflection at $q = 1.625$ Å (Figure 9a) moves only due to the b-axis stretch (nominally corresponding to an interlayer distance), the reflection is (010). The reflections at $q = 0.96$, 2.85, and 3.28 Å (Figure 9b) shift only due to an a-axis stretching and are first-, second-, and third-order reflections of 6.6 Å, which nominally provide the interchain distance. Thus, they are labeled (100), (200),

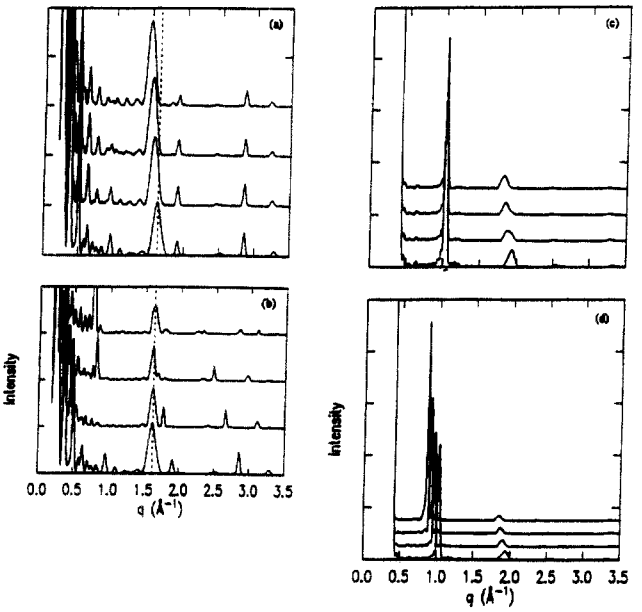

Figure 9. Layer lines of the $n = 2$ structure. The reflection shifts on the equatorial pattern when the structure is stretched along the b and a axes are illustrated in (a) and (b). The counterparts on the second layer line are illustrated in (c) and (d).

and (300). No reflection shifts for both a- and b-axis stretching, indicating the absence of any ($hk0$) type reflection. This is consistent with the fiber pattern (Figure 3). One reflection at $q \sim 1.0$ Å^{-1} appears on the first layer line. It is 2 orders of magnitude weaker than the reflections on the equator and second layer line. It shifts when a stretch is applied to the structure along the a axis. It is, therefore, identified as a (101) reflection. This observation agrees with the experimental measurement (Figure 3). Two reflections at $q = 1.029$ and 1.937 Å^{-1} appear on the second layer line. The former shifts only when a stretch is applied to the structure along the a axis (Figure 9c,d), indicating a (102) reflection. The latter reflection is (112) since it shifts when a stretch is applied along both the a and b axes (Figure 9c,d). The absence of a (012) reflection is consistent with the fiber pattern of Figure 3.

The structure modeled provides quantitative correspondence with the experiments. It reveals the polymorphism in chain conformation, with various ordered chain conformations having comparable energies. While the $n = 2$ conformation is preferred, others may appear as imperfections as yet to be discovered in the solid phase. The occurrence of the $n = 3$ and 4 structures is novel and unexpected and has not yet been confirmed by experiments; thus the present report may serve as a guide to characterize them if they are observed. Although the calculation is by no means optimized, comparison with experiment is quantitative.

IV. Conclusion

The ordered structure of PMDA–ODA in the solid phase is modeled using the CHARMM software package. Considering only empirical potentials between atoms, while ignoring specific interactions such as charge transfer, the model shows quantitative agreement with experiments. Polymorphism in ordered chain conformations is suggested, with $n = 2, 3$, and 4 monomer repeat-unit periodicity along the chain. $n = 2$ and 4 are planar-like structures, and $n = 3$ has a triangular cross-section. The relatively small energy difference between the various ordered conformations partially explains the mesomorphic liquid-crystal-like structure of PMDA–ODA. The lowest energy 3-D structure consists of the $n = 2$ conformation, with the periodicity of a single monolayer along the interplanar packing direction and two monolayer stacks along the edge-on stacking direction. The structure factor corresponding to the meridian reveals eight orders of reflection from (002) to (0,0,16), with a periodic spacing of 16.4 Å. The absence of the (110) and (012) reflections is consistent with experimental observation. The unit cell is orthorhombic and has two chains per cell with $a = 13.20$ Å, $b = 3.86$ Å, and $c = 32.80$ Å, with a density of 1.513 ± 0.028 g/cm^3.

References and Notes

(1) Takahashi, N.; Yoon, D. Y.; Parrish, W. *Macromolecules* **1984**, *17*, 2583.
(2) Bessonov, M. I.; Koton, M. M.; Kudryavtsev, V. V.; Laius, L. A. In *Polyimides: Thermally Stable Polymers*; Consultants Bureau: New York, 1987.
(3) Freilich, S. C.; Gardner, K. H. In *Polyimides: Materials, Chemistry and Characterization*; Feger, C., Khojasteh, M. M., McGrath, J. E., Eds.; Elsevier Science Publishers B.V.: Amsterdam, 1989; p 513.
(4) Factor, B. J.; Russell, T. P.; Toney, M. F. *Phys. Rev. Lett.* **1991**, *66*, 1181.
(5) Saraf, R. F.; Tong, H.-M.; Poon, T. W.; Silverman, B. D.; Ho, P. S.; Rossi, A. R. *J. Appl. Polym. Sci.* **1992**, *46*, 1329.
(6) Numata, S.; Fujisaki, K.; Kinjo, N. *Polymer* **1987**, *28*, 2282.
(7) Numata, S.; Oohara, S.; Fujisaki, K.; Imalzumi, J.; Kinjo, N. *J. Appl. Polym. Sci.* **1986**, *31*, 101.
(8) Numata, S.; Kinjo, N.; Makino, D. *Polym. Eng. Sci.* **1988**, *28*, 906.
(9) Numata, S.; Miwa, T. *Polymer* **1989**, *30*, 1170.
(10) Miwa, T.; Numata, S. *Polymer* **1989**, *30*, 893.
(11) Brook, B. R.; Bruccoleri, R. E.; Olafson, B. D.; States, D. J.; Swaminathan, S.; Karplus, M. *J. Comput. Chem.* **1983**, *4*, 187. QUANTA/CHARMM is a product of Molecular Simulation Corp.
(12) Poon, T. W.; Silverman, B. D.; Saraf, R. F.; Rossi, A. R.; Ho, P. S. *Phys. Rev. B* **1992**, *46*, 11456.
(13) See, for example: Miller, R. L. In *Polymer Handbook*, 2nd ed.; Brandrup, J., Immergut, E. H., Eds.; J. Wiley & Sons: New York, 1975; p III–1.
(14) See, for example: Russell, T. P.; Gugger, H.; Swalen, J. D. *J. Polym. Sci., Polym. Phys. Ed.* **1983**, *21*, 1745.
(15) See, for example: Kaneder, T. *J. Appl. Polym. Sci.* **1986**, *32*, 3151.
(16) Russell, T. P.; Brown, H. R. *J. Polym. Sci., Polym. Phys. Ed.* **1987**, *25*, 1129.
(17) Gardner, K. IVth International Conference on Polyimides, Ellenville, NY, Oct 30–Nov 1, 1991.
(18) Mitchell, G. R.; Windle, A. H. *Polymer* **1984**, *25*, 906.
(19) Saraf, R. F.; Porter, R. S. *J. Polym. Sci., Polym. Phys. Ed.* **1988**, *26*, 1049.